VIP Solar Cells

DOI: 10.1002/anie.201104275

A Trisheteroleptic Cyclometalated Ru^{II} Sensitizer that Enables High Power Output in a Dye-Sensitized Solar Cell**

*Paolo G. Bomben, Terry J. Gordon, Eduardo Schott, and Curtis P. Berlinguette**

The low embodied energy and high power-conversion efficiency (η) over disparate light intensities renders the dye-sensitized solar cell (DSSC)[1,2] a promising alternative to conventional photovoltaic technologies.[3] Significant penetration of the DSSC into the photovoltaic market, however, is hindered predominantly by the long-term stability of dyes and electrolytes under practical conditions.[4–6] The instability of champion (i.e., $\eta > 10\,\%$) dyes (which, until recently,[7] all were derivatives of $[Ru(dcbpy)_2(NCS)_2]$ (**N3**; dcbpy = 4,4′-dicarboxy-2,2′-bipyridine)[2]) in the DSSC is caused primarily by desorption of the dyes from the surface and/or liberation of the NCS^- ligands from the metal centre.[5,6] While the rate of dye desorption from TiO_2 can be manipulated by replacing the $-CO_2H$ moiety with other anchoring groups, this strategy typically compromises electron injection into the TiO_2.[8] An alternative approach is to replace the dcbpy ligands that comprise **N3** with bidentate ligands bearing aliphatic substituents (e.g., Scheme 1 a), which serve to hinder water from reaching the surface to hydrolytically cleave the TiO_2–dye ester linkage.[9] These groups provide the additional benefit of suppressing recombination between the electrolyte and the electrons in TiO_2, thus leading to higher efficiencies (Scheme 1 a).[2]

Chemical strategies for avoiding the labile Ru–NCS bond have been realized recently;[10,11] indeed, we[12] and others[13,14] have now documented remarkably high η values for DSSCs containing NCS^--free Ru^{II} sensitizers. Cyclometalated Ru complexes such as $[Ru^{II}(dcbpy)_2(ppy)]^{1+}$ (ppy = 2-phenylpyridine) provide a versatile platform in this respect because: 1) the highest occupied molecular orbital (HOMO) is extended over the metal and anionic ring thus enabling its modulation through judicious installation of substituents at the $-R_2$ site in Scheme 1 b;[15] and 2) the low-lying excited states, which contain orbital character that resides on the π^* framework of the dcbpy ligand(s), are poised for electron injection into the TiO_2.[10,11,15–18] This scenario leaves open the opportunity to replace one dcbpy with a bidentate ligand capable of suppressing recombination and enhancing the optical properties as per the aforementioned protocol (Scheme 1).[2,19] While we recently demonstrated synthetic access to trisheteroleptic Ru sensitizers (e.g., **1** and **2**; Scheme 2),[20] we learned that removing the acid linkers raises the HOMO level of the sensitizer to potentially compromise dye regeneration. (The HOMO level of the sensitizer must lie lower in energy than the I^-/I_3^- redox couple that resides at approximately +0.5 V vs. normal hydrogen electrode (NHE).[21] Although the HOMO of **1** lies at +0.70 V vs. NHE and therefore meets this criterion,[20] champion Ru-based sensitizers all have oxidation potentials higher than ca. +0.9 V.[2]) We therefore set out to overcome this potential shortcoming by introducing strongly electron-withdrawing $-CF_3$ substituents to the cyclometalating ligand to accommodate efficient dye regeneration. These design elements led to the preparation of **3**—a Ru^{II} complex devoid

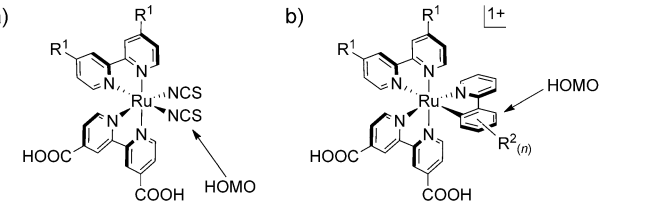

R^1: - delocalized π system enhances light absorption;
- aliphatic groups suppress interaction between electrolyte/H_2O and surface
R^2: - delocalized π system enhances light absorption;
- electron-donating character affects the thermodynamic position of the HOMO

Scheme 1. Molecular design elements that can be manipulated to render high-performance Ru-based DSSC dyes with a) NCS^- groups and b) cyclometalating ligands. The HOMO is localized at the metal and the anionic ligands in both cases as indicated, but is more easily attenuated in the case of the cyclometalated complexes.[10]

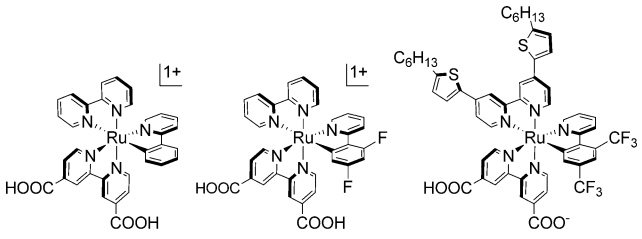

1 **2** **3**

Scheme 2. Trisheteroleptic cyclometalated Ru dyes **1**-**3**.[20]

[*] P. G. Bomben, T. J. Gordon, Prof. C. P. Berlinguette
Department of Chemistry, and the Centre for Advanced Solar Materials, University of Calgary
2500 University Drive NW, Calgary AB, T2N 1N4 (Canada)
E-mail: cberling@ucalgary.ca
E. Schott
Departamento de Ciencias Químicas
Universidad Andres Bello, República 275, Santiago (Chile)

[**] This work was financially supported by the Canada Natural Science and Engineering Research Council (NSERC), Canada Research Chairs, Canadian Foundation for Innovation and Alberta Innovates.

Detailed experimental information including computational methods can be found in the Supporting information for this article, which is available on the WWW under http://dx.doi.org/10.1002/anie.201104275.

of NCS^- groups and bearing aliphatic substituents that can generate high efficiencies in a conventional DSSC. Moreover, we show herein that **3** produces, to the best of our knowledge, the best cell performance to date for a Ru-based dye with a Co-based electrolyte at 1 sun.

The title sensitizer **3** was isolated according to the synthetic approach developed for **1**–**2** (Scheme S1).[20] Briefly, the cyclometalating ligand, ppy-$(CF_3)_2$, which was synthesized by a Negishi coupling of 2-pyridylzinc bromide and 1-bromo-2,4-bis(trifluoromethyl)benzene, $[Ru(C_6H_6)Cl_2]_2$, NaOH, and KPF_6 were reacted to furnish $[Ru(CH_3CN)_4(ppy\text{-}(CF_3)_2)]PF_6$. This complex was then treated with deeb (4,4′-diethylester-2,2′-bipyridine) and dthbpy (2,2′-bis(5-hexylthiophen-2-yl)-2,2′-bipyridine) to give the ethylester intermediate $[Ru(deeb)(dthbpy)(ppy\text{-}(CF_3)_2)]PF_6$, which affords **3** in high purity upon saponification.

The UV/Vis spectrum of **3** reveals a broader and more intense absorption envelope relative to both **1** and **N3** (Figure 1). The absorption spectra of the dyes tethered to

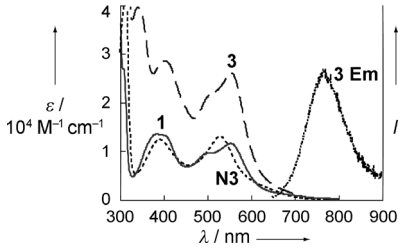

Figure 1. UV/Vis spectra for MeOH solutions of **N3**, **1**, and **3**; the emission spectrum of **3** ($\lambda_{ex} = 555$ nm) is also provided.

TiO_2 follow similar trends, but display a less pronounced difference in intensities, presumably due to the lower surface coverage of **3** (Figure S1). Intense π–π* transitions dominate the spectrum of **3** below 350 nm, while metal-to-ligand charge-transfer transitions comprise the broad bands centered at 404 nm ($\varepsilon = 2.9 \times 10^4\,M^{-1}\,cm^{-1}$) and 555 nm ($\varepsilon = 2.6 \times 10^4\,M^{-1}\,cm^{-1}$). These assignments were corroborated by DFT, which predicts the two lowest-energy bands to contain transitions from a metal-based HOMO-1 level to lowest unoccupied molecular orbital (LUMO) and LUMO + 1 levels that have orbital character localized to the polypyridyl ligands (Figure S2). The shoulder at approximately 660 nm for **3** is predicted by DFT to be a HOMO to LUMO transition characterized by a low oscillator strength arising from the orthogonality of the constituent orbitals; however, this band may also be due to the direct population of the ^{3}MLCT state.[22] The intensities of the low-energy absorption bands of **3** are relatively higher than those of **1** and **N3** due to the presence of the thiophene units. Importantly, light absorption by **3** occurs beyond 700 nm even with the electron-withdrawing $-CF_3$ groups present.

The cyclic voltammogram of **3** in DMF reveals a reversible one-electron oxidation at + 0.99 V vs. NHE and a reversible ligand-based reduction wave at −1.17 V vs. NHE (Figure S3). (For comparison, the first oxidation potentials for **1** and **2** occur at + 0.70 and + 0.93 V, respectively.) The E_{0-0} energy of 1.84 eV for **3** extracted from the intersection of the absorption and emission profiles[23] enables a determination of the excited-state oxidation potential $E(S^+/S^*)$ to be −0.85 V—a value that is appropriately positioned for electron injection into the TiO_2 conduction band ($E_{CB} \approx -0.5$ V vs. NHE).[24]

Photovoltaic data was recorded on DSSCs containing **3** with electrolytes relying on either the I^-/I_3^- (denoted EL1) or Co^{III}/Co^{II} (denoted EL2) redox couples (Table 1). Data for

Table 1: Photovoltaic data obtained under AM1.5 irradiation.[a]

Entry	Dye	El[b]	Light Level[c]	V_{oc} [V]	J_{sc} [mA cm^{-2}]	*FF*	η [%]
1	**1**	EL1	1	0.63	9.7	0.66	4.1
2	**N3**	EL1	1	0.65	13.3	0.73	6.3
3	**3**	EL1	1	0.66	16.3	0.68	7.3
4	**3**	EL1	0.5	0.64	8.6	0.74	8.3
5[d]	**3**	EL1	0.5	0.66	9.6	0.68	8.8
6[e]	**3**	EL1	1	0.73	14.3	0.66	6.9
7	**3**	EL2	1	0.72	11.8	0.64	5.5
8[d]	**3**	EL2	1	0.78	13.1	0.61	6.2
9	**N3**	EL2	1	0.49	3.8	0.51	0.96

[a] DSSC substrates consist of a 12 μm TiO_2 active layer and 3 μm TiO_2 scattering layer unless otherwise specified. [b] El = electrolyte; EL1: BMII (1-butyl-3-methylimidazolium iodide) (0.6 M), I_2 (0.06 M), NaI (0.1 M), *t*BP (4-*tert*-butylpyridine) (0.5 M), GuSCN (guanidinium thiocyanate) (0.1 M) in MeCN; EL2: $[Co(bpy)_3](PF_6)_2$ (0.21 M), $[Co(bpy)_3](PF_6)_3$ (0.033 M), $NaClO_4$ (0.1 M), *t*BP (0.2 M) in MeCN. [c] Light intensity measured in suns. [d] Data recorded on same cell as previous entry without a mask. [e] Substrate consists of a 6 μm TiO_2 active layer and 3 μm TiO_2 scattering layer.

devices containing **1** and **N3** are also provided as a benchmark (Entries 1–2, Table 1). While our devices with EL1 reach $\eta = 6.3\,\%$ for **N3**, a markedly lower value is obtained for **1**, which is presumably due to an oxidation potential (i.e., + 0.70 V[20]) that is inappropriate for efficient dye regeneration. The higher oxidation potential (and slightly enhanced absorbance) of **3**, however, leads to a stark improvement in cell performance among the series (Entry 3, Table 1; Figure 2). Indeed, efficiencies approaching 9 % were obtained for cells measured at lower light intensities and/or without a mask (Entries 4–5, Table 1).

The superior cell performance of **3** is manifested in the higher short-circuit photocurrent density (J_{sc}; 16.3 mA cm^{-2}), which arises from the thiophene groups enhancing the

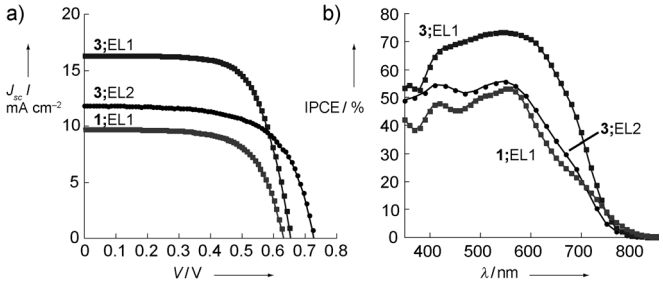

Figure 2. a) Current–voltage curves recorded under AM1.5 conditions and b) IPCE data for DSSCs sensitized with **1** and **3**. Squares (■) and circles (●) represent cells measured with EL1 and EL2, respectively (TiO_2: 12 μm active and 3 μm scattering layers).

absorbance profile and the alkyl groups suppressing recombination. This claim is corroborated by: 1) normalized incident-photon-to-current efficiency (IPCE) measurements, which display an enhanced external quantum efficiency between 600–700 nm for **3** (Figure S4); and 2) Nyquist plots of cells measured in the dark at the voltage corresponding to their V_{oc} (Figure S5). (A transmission line model (as depicted in Figure S6) was applied to the electrochemical impedance spectroscopy (EIS) data; the results are summarized in Table S1.[25]) For conventional cells (i.e., EL1 and a 12 μm TiO_2 active layer), the electron-transport resistance in TiO_2 was found to be highest for **1** (64 Ω) and lowest for **3** (11 Ω). Moreover, cells containing **3** had the highest resistance (30 Ω) to electron recombination with EL1 and thus the longest electron-diffusion length, L_n.

Given the superior absorbance of **3**, we investigated the performance of cells using thinner TiO_2 films (Entry 6, Table 1). Despite a two-fold reduction in the film thickness of the substrate, the J_{sc} was lowered by only 12% to 14.3 mA cm^{-2}. This diminution in current was countered by an 11% increase in V_{oc} to 0.73 V, which offsets the decrease in photocurrent to afford a reasonably high η value of 6.9%. EIS data indicates that the increase in V_{oc} emanates from lower recombination arising from improved charge collection (e.g., a low transport resistance of 2 Ω coupled to a larger charge-transfer resistance with the electrolyte of 33 Ω), thereby resulting in a cell that exhibits minor losses in performance compared to the analogous cells with thicker substrates.

Recent reports have highlighted electrolytes that rely on the Co^{III}/Co^{II} redox shuttle and that can produce high η values for organic dyes;[26–28] however, a similar performance rating with Ru-based dyes at 1 sun has not yet been demonstrated; for example, 3.9% using the $[Co(dbbip)_2]^{2+/3+}$ redox couple (dbbip = 2,6-bis(1′-butylbenzimidazol-2′-yl)pyridine) with **Z907**.[29] Because the electronic geometry of the HOMO for **3** differs from that of dyes bearing NCS^- ligands (e.g., **N3**, **Z907**), we were curious if the interaction with an electrolyte derived from $[Co(bpy)_3]^{2+/3+}$ (e.g., EL2) could achieve a higher cell performance. This line of inquiry was rewarded by the observation that a DSSC containing **3** reached $\eta = 5.5\%$ (Entries 7 and 8), which appears to be the highest value obtained for any Ru-based dye with a Co-based electrolyte at 1 sun. To date, the highest efficiency for a Ru-based dye using $[Co(bpy)_3]^{2+/3+}$ is 1.3%;[30] we were only able to obtain a cell efficiency of 0.96% with **N3** (Entry 9, Table 1). Note that the high η and IPCE values (e.g., 50% over 400–600 nm) for **3** were obtained without the use of blocking layers.[30,31] We observe a much larger Warburg feature in our EIS measurements for EL2 than for EL1 (Figure S5), which we ascribe to mass-transport limitations;[32] thus, investigations are underway to optimize cells of **3** with cobalt electrolytes using thinner TiO_2 films.

This study discloses the first high-efficiency trisheteroleptic cyclometalated Ru sensitizer. The efficacy of this NCS^--free dye is a consequence of a sufficiently high Ru^{III}/Ru^{II} redox potential achieved by installing electron-withdrawing groups at R_2, thereby enhancing light absorption by placing thiophenes at R_1, and suppressing charge recombination with terminal alkyl groups on said thiophenes. A performance of 7.3% was achieved at AM1.5 and 8.3% at half that light intensity. We also demonstrate that a noncorrosive cobalt electrolyte achieves an efficiency of 5.5% and a photocurrent of 11.8 mA cm^{-2} under full sun illumination. An examination of the long-term stability of **3** in the DSSC is underway. These results provide an important breakthrough for making high-performance cyclometalated Ru dyes for use in the DSSC.

Received: June 21, 2011
Published online: August 30, 2011

Keywords: cobalt · donor–acceptor systems · energy conversion · ruthenium · sensitizers

[1] B. O'Regan, M. Grätzel, *Nature* **1991**, *353*, 737–740.
[2] A. Hagfeldt, G. Boschloo, L. Sun, L. Kloo, H. Pettersson, *Chem. Rev.* **2010**, *110*, 6595–6663.
[3] D. Shi, N. Pootrakulchote, R. Li, J. Guo, Y. Wang, S. M. Zakeeruddin, M. Grätzel, P. Wang, *J. Phys. Chem. C* **2008**, *112*, 17046–17050.
[4] L. Wang, X. Fang, Z. Zhang, *Renewable Sustainable Energy Rev.* **2010**, *14*, 3178–3184.
[5] P. T. Nguyen, A. R. Andersen, E. M. Skou, T. Lund, *Sol. Energy Mater. Sol. Cells* **2010**, *94*, 1582–1590.
[6] P. T. Nguyen, B. X. T. Lam, A. R. Andersen, P. E. Hansen, T. Lund, *Eur. J. Inorg. Chem.* **2011**, 2533–2539.
[7] T. Bessho, S. Zakeeruddin, C. Y. Yeh, E. G. Diau, M. Grätzel, *Angew. Chem.* **2010**, *122*, 6796–6799; *Angew. Chem. Int. Ed.* **2010**, *49*, 6646–6649.
[8] E. Galoppini, *Coord. Chem. Rev.* **2004**, *248*, 1283–1297.
[9] P. Wang, C. Klein, R. Humphry-Baker, S. M. Zakeeruddin, M. Grätzel, *J. Am. Chem. Soc.* **2005**, *127*, 808–809.
[10] P. G. Bomben, K. C. D. Robson, P. A. Sedach, C. P. Berlinguette, *Inorg. Chem.* **2009**, *48*, 9631–9643.
[11] S. H. Wadman, J. M. Kroon, K. Bakker, M. Lutz, A. L. Spek, G. P. M. van Klink, G. van Koten, *Chem. Commun.* **2007**, 1907–1909.
[12] K. C. D. Robson, B. Sporinova, B. D. Koivisto, T. Baumgartner, A. Yella, Nazeeruddin, M. K., M. Grätzel, C. P. Berlinguette, *Inorg. Chem.* **2011**, *50*, 5494–5508.
[13] C.-C. Chou, K.-L. Wu, Y. Chi, W.-P. Hu, S. J. Yu, G.-H. Lee, C.-L. Lin, P.-T. Chou, *Angew. Chem.* **2011**, *123*, 2102–2106; *Angew. Chem. Int. Ed.* **2011**, *50*, 2054–2058.
[14] T. Bessho, E. Yoneda, J.-H. Yum, M. Guglielmi, I. Tavernelli, H. Imai, U. Rothlisberger, M. K. Nazeeruddin, M. Grätzel, *J. Am. Chem. Soc.* **2009**, *131*, 5930–5934.
[15] P. G. Bomben, B. D. Koivisto, C. P. Berlinguette, *Inorg. Chem.* **2010**, *49*, 4960–4971.
[16] S. H. Wadman, M. Lutz, D. M. Tooke, A. L. Spek, F. Hartl, R. W. A. Havenith, G. P. M. van Klink, G. van Koten, *Inorg. Chem.* **2009**, *48*, 1887–1900.
[17] B. D. Koivisto, K. C. D. Robson, C. P. Berlinguette, *Inorg. Chem.* **2009**, *48*, 9644–9652.
[18] C.-J. Yao, L.-Z. Sui, H.-Y. Xie, W.-J. Xiao, Y.-W. Zhong, J. Yao, *Inorg. Chem.* **2010**, *49*, 8347–8350.
[19] S. Ardo, G. J. Meyer, *Chem. Soc. Rev.* **2009**, *38*, 115–164.
[20] P. G. Bomben, K. D. Thériault, C. P. Berlinguette, *Eur. J. Inorg. Chem.* **2011**, 1806–1814.
[21] All redox potentials are reported vs a normal hydrogen electrode (NHE) in this study.
[22] N. Hirata, J. J. Lagref, E. J. Palomares, J. R. Durrant, M. K. Nazeeruddin, M. Gratzel, D. Di Censo, *Chem. Eur. J.* **2004**, *10*, 595–602.
[23] Excitation of the lowest-energy peak of **3** produces a weak emission band centred at 767 nm; Figure 1.

[24] M. Grätzel, *Nature* **2001**, *414*, 338 – 344.
[25] F. Fabregat-Santiago, J. Bisquert, G. Garcia-Belmonte, G. Boschloo, A. Hagfeldt, *Sol. Energy Mater. Sol. Cells* **2005**, *87*, 117 – 131.
[26] S. M. Feldt, E. A. Gibson, E. Gabrielsson, L. Sun, G. Boschloo, A. Hagfeldt, *J. Am. Chem. Soc.* **2010**, *132*, 16714 – 16724.
[27] D. Zhou, Q. Yu, N. Cai, Y. Bai, Y. Wang, P. Wang, *Energy Environ. Sci.* **2011**, *4*, 2030 – 2034.
[28] H. N. Tsao, C. Yi, T. Moehl, J.-H. Yum, S. M. Zakeeruddin, M. K. Nazeeruddin, M. Grätzel, *ChemSusChem* **2011**, *4*, 591 – 594.
[29] H. Nusbaumer, S. M. Zakeeruddin, J.-E. Moser, M. Grätzel, *Chem. Eur. J.* **2003**, *9*, 3756 – 3763.
[30] B. M. Klahr, T. W. Hamann, *J. Phys. Chem. C* **2009**, *113*, 14040 – 14045.
[31] J. W. Ondersma, T. W. Hamann, *J. Phys. Chem. C* **2010**, *114*, 638 – 645.
[32] J. J. Nelson, T. J. Amick, C. M. Elliott, *J. Phys. Chem. C* **2008**, *112*, 18255 – 18263.

